

Tight binding studies of strained Ge/Si(001) growth

K. Li¹, D.R. Bowler* and M.J. Gillan

*Department of Physics and Astronomy, University College London, Gower Street,
London WC1E 6BT, UK*

Abstract

Experimental observations of the growth of more than one monolayer of Ge on Si(001) show a progression of effects beyond the $(2 \times N)$ reconstruction which is seen at submonolayer coverages: a reduction in the value of N with coverage; formation of straight trenches of missing dimer vacancies; and formation of the $(M \times N)$ “patch” structure. We present tight binding calculations which investigate the energetics and geometries associated with these effects, and extend our earlier treatment of formation energies for reconstructions with different stoichiometries to the case of several layers of Ge. The results provide explanations for the various effects seen, and are in good agreement with experimental observations.

Key words: Computer simulations, surface stress, silicon, germanium, semiconductor-semiconductor heterostructures

1 Introduction

Understanding the relationship between strain and the formation of nanostructures is extremely important as practical nanoelectronic devices are sought. The growth of Ge on Si(001) is particularly interesting in this context, not only because of the small, three dimensional features which form at high coverage (the so-called “hut clusters” [1]) but also because of the direct compatibility with standard group IV semiconductor technology. In this paper, we

* Corresponding author

Email addresses: khli@xmu.edu.cn (K. Li), david.bowler@ucl.ac.uk (D.R. Bowler), m.gillan@ucl.ac.uk (M.J. Gillan).

URL: <http://www.cmp.ucl.ac.uk/~drb/research.html> (D.R. Bowler).

¹ Permanent Address: Physics Department, Xiamen University, Xiamen, 361005, P.R.China

present tight binding calculations of various aspects of Ge growth on Si(001) for coverages between one and three monolayers (ML) of Ge. This work follows naturally from our previous paper[2], where we studied the $(2 \times N)$ reconstruction which forms at sub-monolayer coverages using first principles electronic structure techniques.

As the coverage of Ge on Si(001) approaches 1ML, it forms the well-known $(2 \times N)$ reconstruction, where regularly spaced missing dimers appear in the surface; experimental observations of N show that it typically lies between 8 and 12, with the spacing dependent on growth source (gas source, e.g. GeH₄, or solid source) and conditions (growth rate and temperature)[3,4]. As the thickness of the deposited layer increases, various further effects are seen on this reconstruction, again depending on growth source and conditions for their onset: the value of N decreases[4,5,6]; the missing dimers align in neighbouring dimer rows to form straight trenches[5,6]; a new, patch-like reconstruction with a double periodicity (called the $(M \times N)$ reconstruction) forms (illustrated in Fig. 1)[3,7,8]; the roughness of step edges changes (with the different step types eventually becoming equally rough, leading to steps running along the elastically soft (100) and (010) directions)[5]; and finally three dimensional structures such as “hut” pits and clusters form[1,9]. We shall investigate the first three of these phenomena in this paper.

The modelling of the formation of straight trenches and the $(M \times N)$ reconstruction requires large unit cells, while the comparisons we are performing require a quantum mechanical technique for accuracy (for instance, to correctly model the dimer buckling on the surface). We have chosen to use an $\mathcal{O}(N)$ (or linear scaling) tight binding technique to meet these criteria[10] (this is a technique where the computer effort required scales linearly with the system size at the expense of an approximation, rather than with the cube of the system size, as is the case for standard techniques, referred to as “diagonalisation”). However, this introduces two levels of approximation: the first, inherent in the tight binding parameterisation; the second, in the use of an $\mathcal{O}(N)$ method. We test these approximations separately. First, we test the parameterisation by comparing the results of exact diagonalisation to *ab initio* results. Second, we check the accuracy of the $\mathcal{O}(N)$ technique against the exact diagonalisation tight binding results. This gives us a clear idea of what errors are introduced and where. Starting from the $(2 \times N)$ reconstruction, we investigate first the dependence of the value of N on the depth of the Ge layers. We then calculate the energetics of kinks in trenches of missing dimers with increasing Ge depth, in order to understand the formation of straight trenches of missing dimers. Finally we address the $(M \times N)$ reconstruction, calculating minimum energy values of M for a fixed value of N . In all of the above calculations, we will also address the question of an appropriate energy to use for Ge dimers when comparing reconstructions of different stoichiometry, which is closely related to the problem of finding an appropriate chemical

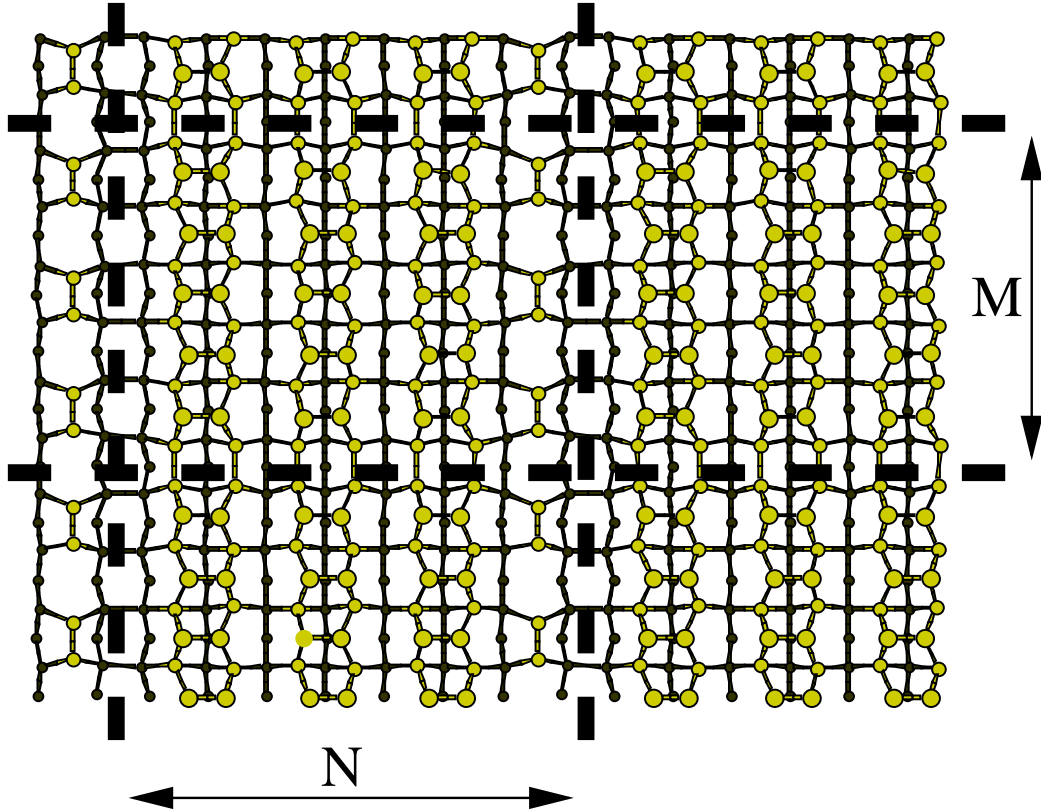


Fig. 1. A top-down view of the $(M \times N)$ surface for two layers of Ge on Si (only the top four layers are shown for simplicity; the Ge is shown as light circles, with the top layer larger than the second layer, while Si is shown as dark circles). The underlying $(2 \times N)$ reconstruction has dimer rows running across the page horizontally, while the top-layer $(M \times 2)$ reconstruction has dimer rows running vertically. For this cell, $N = 8$ (equivalent to three dimer rows and a missing row in the top layer) and $M = 6$ (equivalent to five dimers and a missing dimer in the top layer).

potential for Ge.

The previous work in this area only addressed the $(2 \times N)$ reconstruction, and investigated the dependence of N on depth of Ge using empirical potentials, such as the Stillinger-Weber and modified Keating forms [11,12,13]. These studies found results in broad agreement with experiment, and our previous work[2] provides support for the mechanisms suggested by these empirical studies. We note that intermixing of Si and Ge may well occur during experimental growth[4,6], though this depends on experimental conditions, and is thought to be largely suppressed after one monolayer of Ge. The likely effect would be to reduce the surface strain somewhat; we have chosen not to account for intermixing for three reasons. First, there are experimental results available for situations where intermixing is almost entirely suppressed, with which we can make direct contact. Second, it adds significant additional complication to the problem, where we are trying to find the underlying mechanisms.

Third, the effects are likely to be relatively small. Indeed, in previous empirical work[13], the authors concluded that the Ge/Si interlayer mixing could not be substantial. In a recent detailed *ab initio* study of intermixing[14], it was shown that, while Ge can penetrate to the fourth layer, this is likely to be at the level of a few percent at a typical low growth temperature (e.g. 500°C). Hence, we neglect this effect in the present work.

The rest of the paper proceeds as follows: in the next section we review the details of the computational techniques used, consider the question of what energies to use when comparing reconstructions of different periodicity (and hence stoichiometry) and test the accuracy of our methods; after this, we present our results for the different situations considered (the $(2 \times N)$ reconstruction with increasing Ge depth; trench kinking with increasing Ge depth; the $(M \times N)$ reconstruction), and we finish with a discussion of the results.

2 Computational Details

2.1 Tight Binding Parameters

The tight binding technique has been discussed elsewhere in detail[15], as have the ideas and implementation of $\mathcal{O}(N)$ techniques[10]. We used a parameterisation for Si-Si bonds (and Si-H bonds for termination) specifically designed for and tested extensively on the Si(001) surface[16], and a parameterisation for Ge-Ge and Ge-Si bonds again tested on the Si(001) surface, and fitted to reproduce the experimental Ge lattice constant (giving a lattice mismatch of 4% between Ge and Si)[17]. We used the OXON code to perform exact diagonalisations, and the DENSEL code (an implementation[18] of the auxiliary density matrix (ADM) technique[19]) for linear scaling calculations.

We work with periodic boundary conditions, simulating a surface via a slab with a vacuum gap equivalent to eight atomic layers of Si. In all cases, the slab modelled was ten atomic layers deep, with the bottom layer terminated in hydrogen. The length and width used depended on the calculations: for the $(2 \times N)$ calculations, cells were one dimer row wide, and ranged from four to twelve dimers long (from 94 to 286 atoms); for trench kinking calculations, they were between two and six dimer rows wide and eight (1 or 2ML Ge) or six (3ML Ge) dimers long (from 284 atoms to 1,140 atoms); and for the $(M \times N)$ reconstructions, they were typically six dimer rows wide and eight dimers long (around 1,100 atoms). We investigated the importance of substrate relaxation, and found that in most cases (in all cases with 2 or more monolayers of Ge on Si(001)) allowing four layers of silicon below the Ge to relax gave energy convergence to within a few meV (and presented the same amount of substrate

relaxation below the Ge). For the detailed comparison of one monolayer of Ge on Si(001) presented below, we found that allowing seven layers of silicon to relax was important. The reason for this lies in the rebonding of the second layer atoms across the gap where the dimer is missing. When these atoms are silicon, they are stretched across the gap, and require significant depth for relaxation of strain. When they are germanium, the rebonding helps to alleviate the mismatch with the silicon substrate, and less depth is required.

When using exact diagonalisation to test the parameterisation involving Ge against earlier DFT results, we used a $4 \times 2 \times 1$ Monkhorst-Pack \mathbf{k} -point mesh[20], which we found converged total energies to within 2 or 3 meV. When performing the linear scaling calculations, we had to choose a cutoff on the density matrix, which in the DENSEL code is typically specified as a number of hamiltonian-range hops. Previous work has shown that, for semiconductors and insulators, forces and energy differences are well converged at 3 hops (roughly 6 Å in Si) and completely converged at 5 hops (roughly 10 Å in Si)[21]. We present detailed calculations for the energy of one monolayer of Ge in the $(2 \times N)$ reconstruction below (in section 2.3), but the conclusion is that 3 hops is an appropriate compromise between accuracy and CPU time.

2.2 Comparing different stoichiometries

In our previous paper[2], where we presented *ab initio* calculations of the $(2 \times N)$ reconstruction for sub-monolayer coverages of Ge, we gave detailed arguments for the energy to be used for Ge dimers when comparing reconstructions of different periodicity and hence stoichiometry. This energy (which is closely related to a chemical potential) is extremely important when making contact with the experimentally observed values of N and M , which is one of the aims of this paper. We will briefly recall the statistical mechanical arguments used before, and then extend them to the rather different situations found in this work.

We are assuming that the surface is in thermal equilibrium, which means of course that we are ignoring kinetic effects — an assumption that will be discussed in Sec. 4. Then, for a given number of Ge atoms on the surface, the probability of finding them in a particular arrangement Γ will be proportional to $\exp(-E_\Gamma/k_B T)$, with E_Γ the energy for the arrangement Γ .

We only need to know how E_Γ varies from one arrangement to another since we are considering a *fixed* number of atoms. However, it will be helpful to use one specific arrangement as a “reference” arrangement; we choose this to be all Ge atoms paired into dimers and arranged in a perfect, lattice-matched monolayer covering a certain area of the surface. The shape is unimportant, but it is easier

to consider a rectangle. We now consider forming regular arrays of missing dimer trenches by removing dimers from the monolayer and replacing them at the edges of the island, and allowing the system to relax. It is convenient to split this process into two parts: (i) fetch an appropriate number of Ge dimers (equivalent to the number to be removed) from infinity and place them at the boundary of the layer; (ii) remove the appropriate Ge dimers to form missing dimer trenches and relax the system. We now calculate the quantity $\zeta(N)$, which is the energy change per Ge dimer in going from a perfect layer to a periodically reconstructed one. It is given by[2]:

$$\zeta(N) = \frac{(E_f(N) + E_p)}{(N - 1)}, \quad (1)$$

where $E_f(N)$ is the formation energy of fully relaxed missing dimers in the top layer with spacing N (defined as the energy difference between a relaxed surface with a missing dimer reconstruction and a surface with a perfect top Ge layer), and E_p is the energy for a Ge dimer in the reference system (a perfect layer — the energy is defined as the difference per Ge dimer between a surface with a perfect top Ge layer, and the surface formed by removing the top layer of Ge and reconstructing and relaxing). By finding the minimum value of $\zeta(N)$ while varying N , we can find the expected value of N . It should be noted that if $\zeta(N)$ is *positive*, then the reconstruction is *less* stable than a perfect monolayer of Ge (which was chosen as the reference system).

Now we consider how to generalise this argument to the systems considered in this paper. There are four comparisons that we will make:

- (1) The $(2 \times N)$ reconstruction, on multiple layers of Ge (compared to experiment) (Sec. 3.1)
- (2) The energy of missing dimer trenches with and without disorder (compared to each other) (Sec. 3.2)
- (3) The $(M \times N)$ reconstruction, with multiple layers of Ge (compared to experiment) (Sec. 3.3)
- (4) The energies of $(2 \times N)$ and $(M \times N)$ reconstructions on the same number of layers of Ge (compared to each other) (Sec. 3.4)

For the second of these (the energetics of disorder in missing dimer trenches), we do not need to concern ourselves with compensation for different amounts of Ge, as there is no variation in period, just in arrangements of missing dimers. For the other three, we need to identify appropriate energies to use when making the comparisons discussed above, as well as the physical situation we are dealing with.

The $(2 \times N)$ reconstruction on multiple layers of Ge This is possibly the simplest case to deal with. To be clear, we have a system composed of a Si substrate, with θ layers of Ge on top, only the top layer of which has a missing dimer reconstruction (in other words we have $\theta - 1$ full layers of Ge on top of Si as our substrate). Then we use the same argument as we used for sub-monolayer coverages of Ge on Si(001) — i.e. we consider a pool of Ge on top of $\theta - 1$ full layers of Ge on Si, and examine different arrangements that we could make with it, calculating $\zeta(N)$ for each. The energy that we require for comparisons is then the energy difference per Ge dimer between θ full layers of Ge on Si, and $\theta - 1$ full layers of Ge on Si, which we call $E_p(\theta)$, where θ is the coverage (or number of layers).

The $(M \times N)$ reconstruction on multiple layers of Ge The easiest energy to use for this case is little different to that used above; we assume that we have $\theta - 2$ full layers of Ge on top of Si, and then a further layer of Ge with a $(2 \times N)$ reconstruction (the $\theta - 1^{\text{th}}$ layer). This acts as our substrate; since there is a $(2 \times N)$ reconstruction, and the dimer row direction rotates by 90° with each layer, we must form finite width strips of Ge on this substrate (where the width is $N/2 - 1$ dimer rows) to make an $(M \times N)$ reconstruction. We now consider our pool of Ge as divided into strips, and make different arrangements with that, now calculating $\zeta(M)$ for each. The energy required is then just the energy difference per Ge dimer between perfect strips of Ge on a $(2 \times N)$ reconstructed surface with $\theta - 1$ layers of Ge and the $(2 \times N)$ surface reconstructed surface with $\theta - 1$ layers of Ge, which we call $E_{\text{pstrip}}(\theta)$, where again θ is the coverage (or number of layers).

The $(2 \times N)$ and $(M \times N)$ reconstructions on multiple layers of Ge

It is easiest to compare these reconstructions by comparing their stabilities relative to the perfect surface, which requires compensation for the missing Ge. For the $(2 \times N)$ reconstruction, this requires only $E_p(\theta)$, which has already been calculated above. For the $(M \times N)$ reconstruction, we need to perform a little more work, but only using quantities that we already have — the energy of Ge dimers in a perfect layer of a given thickness, $E_p(\theta)$ (both θ and $\theta - 1$ will be required: $\theta - 1$ to compensate for the missing dimer trench in the underlying $(2 \times N)$ reconstruction, and θ to compensate for the missing rows of dimers in the top layer), as well as $E_{\text{pstrip}}(\theta)$.

2.3 Testing Approximations

We now consider the errors introduced by the two approximations that we use: tight binding, rather than full *ab initio* theory; and the cutoff on the density

matrix used in the linear scaling technique. In figure 2, we present the results for $\zeta(N)$ (defined above in equation 1) for sub-monolayer coverages of Ge on Si(001). The main graph shows the results found using exact diagonalisation plotted with the DFT results from our earlier paper[2], while the inset graph shows the $\mathcal{O}(N)$ results plotted with the exact diagonalisation results. The technique used to calculate $\zeta(N)$ is discussed in detail in Ref. [2] and briefly above in Sec. 2.2.

Considering the *ab initio* and tight binding exact diagonalisation results first, we can see that the agreement is good for large N , but that at $N = 4$ in particular there is a considerable discrepancy. However, the reason for this is not due to the approximation made in using tight binding. The lattice mismatch of the *ab initio* results[2] is too large (calculated to be 5.7% as opposed to the experimental and (fitted) tight binding value of 4%) which will increase any strain-related effects; also, the *ab initio* calculations allowed only the top four layers of the slab to relax. Using the same conditions as the *ab initio* calculations (top four layers relaxing, and rescaling the tight binding parameters to create a 5.7% lattice mismatch) we find $\zeta(N = 4) = 0.054$ eV, where the *ab initio* value is 0.079 eV, which is in much better agreement. This suggests that the discrepancy between the tight binding and *ab initio* results for small N is in large part due to the different lattice parameter and simulation conditions, and that the tight binding parameterisation has introduced only minor inaccuracies relative to the *ab initio* calculations.

We must also consider the effect of cutting off the density matrix (the essential approximation in creating an $\mathcal{O}(N)$ method) on the tight binding results. Data from the DENSEL calculations for two different density matrix cutoffs (three and five hamiltonian range hops, which correspond roughly to 6 Å and 10 Å) and the exact diagonalisation are shown in the inset to Fig. 2. We can see that, at 5 hops, the $\mathcal{O}(N)$ results and the exact diagonalisation results are in almost exact agreement, while at 3 hops the overall shape of the curve is reproduced well, though the exact numerical values are a little high. However, these results are sufficiently accurate for our purposes, and we will use a 3 hop cutoff in all calculations in the paper. These results are in excellent agreement with previous work[21] which suggested that energy differences were completely converged at 5 hops and well converged at 3 hops.

3 Results

In this section we present results for a series of increasingly complex reconstructions for coverages of Ge on Si(001) that exceed 1ML: calculations of the value of N for the $(2 \times N)$ reconstruction; calculations of the energy of kinks in the missing-dimer trenches for this reconstruction (for 1ML as well as more

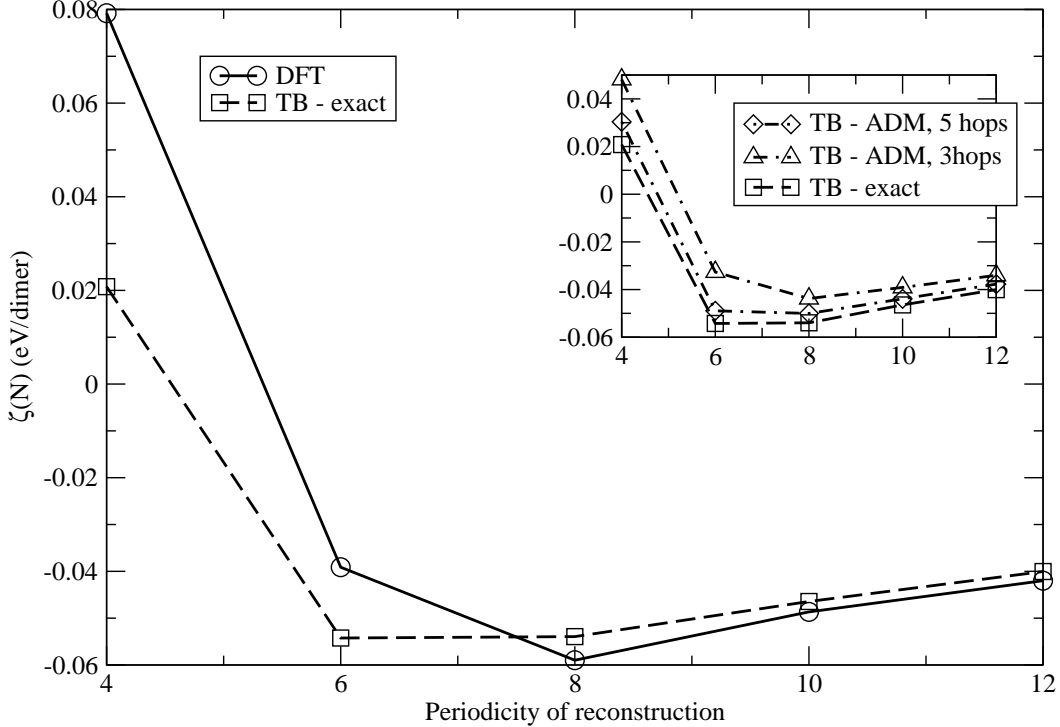


Fig. 2. The energy change per Ge dimer to form a periodically reconstructed surface from a perfect one, $\zeta(N)$, for the $(2 \times N)$ Ge/Si(001) surface plotted against N , calculated using DFT and exact diagonalisation tight binding. Inset: the same quantities calculated using exact diagonalisation tight binding and $\mathcal{O}(N)$ tight binding (ADM) with density matrix cutoffs of 5 and 3 hamiltonian-range hops. See text for a detailed discussion.

than 1ML); and finally the $(M \times N)$ “patch” reconstruction.

3.1 The $(2 \times N)$ reconstruction for more than 1ML

Under certain growth conditions, the $(2 \times N)$ reconstruction is seen to persist when more than one monolayer of Ge has been deposited. This results in a more strained layer, and the appearance of the reconstruction changes: the spacing of the missing dimer trenches decreases, and the trenches become straighter. In this section, we investigate the effect on periodicity, while in the next section (Sec. 3.2) we model the straightening of the trenches.

The energy used for comparisons between different periodicities, $E_p(\theta)$, is -10.35 eV/dimer for $\theta = 1$ ML, -10.08 eV/dimer for $\theta = 2$ ML, and -10.11 eV/dimer for $\theta = 3$ ML. The small increase in this energy from 2ML to 3ML is surprising, but can be attributed to relaxation effects in the substrate (the third layer of Ge allows more relaxation than might be expected).

The results for different Ge ML coverage are given in table 1 and Figure 3.

Table 1

Formation energy of $(2 \times N)$ reconstruction for the Ge/Si(100) surface relative to perfect Ge/Si(100) surface and $\zeta(N)$ for increasing Ge coverage (described above in Sec. 2.2). Energies were obtained using ADM.

	θ_{Ge} (ML)	4	6	8	10	12
E_f	1	10.492	10.184	10.041	9.995	9.974
$\zeta(N)$	1	0.048	-0.033	-0.044	-0.039	-0.034
E_f	2	9.738	9.478	9.393	9.360	9.345
$\zeta(N)$	2	-0.115	-0.121	-0.099	-0.080	-0.067
E_f	3	9.544	9.246	9.151	9.116	9.101
$\zeta(N)$	3	-0.189	-0.173	-0.137	-0.111	-0.092

As shown in the figure, the optimal N value decreases when Ge coverage increases from 1ML to 2 ML, and again from 2 ML to 3 ML. This result indicates that increasing the Ge coverage results in more and more vacancies to release evolving stress and reduce strain energy. Figure 3 also shows that the increase in energy with N becomes steeper at the deeper coverages, indicating that the statistical distribution of N would become narrower with increasing Ge coverage (since the larger values of N become more expensive energetically), as also shown by STM[3]. These results are broadly in agreement with what would be expected for an increasingly strained surface, and point towards the next stage in stress relief in this system: three dimensional islands (often known as “hut clusters”). The value of $N = 4$ (or smaller) for 3ML is a little surprising — it is rather smaller than seen in experiment, or reported previously in modelling. The discrepancy with previous modelling is not surprising, as we use a different method of comparison with experiment. The discrepancy with experiment is somewhat more troubling, and will be discussed more in Section 4.

3.2 Ordering the $(2 \times N)$ trenches

In experiments where the $(2 \times N)$ reconstruction persists with increasing Ge coverage, as well as gradually reducing the periodicity N , the missing dimers become more ordered — i.e. they line up to form straight trenches. The obvious explanation for this is that it becomes energetically more favourable for the missing dimers to align with increasing Ge depth, and it is this phenomenon that we investigate here. Our strategy is to calculate the energy cost of disordering a trench of missing dimers as a function of the depth of Ge on the surface. We will introduce isolated kinks into straight trenches (i.e. a displacement of one or more dimers as we go from one dimer row to an adjacent one, as illustrated in Fig. 4) and calculate the energy difference between this

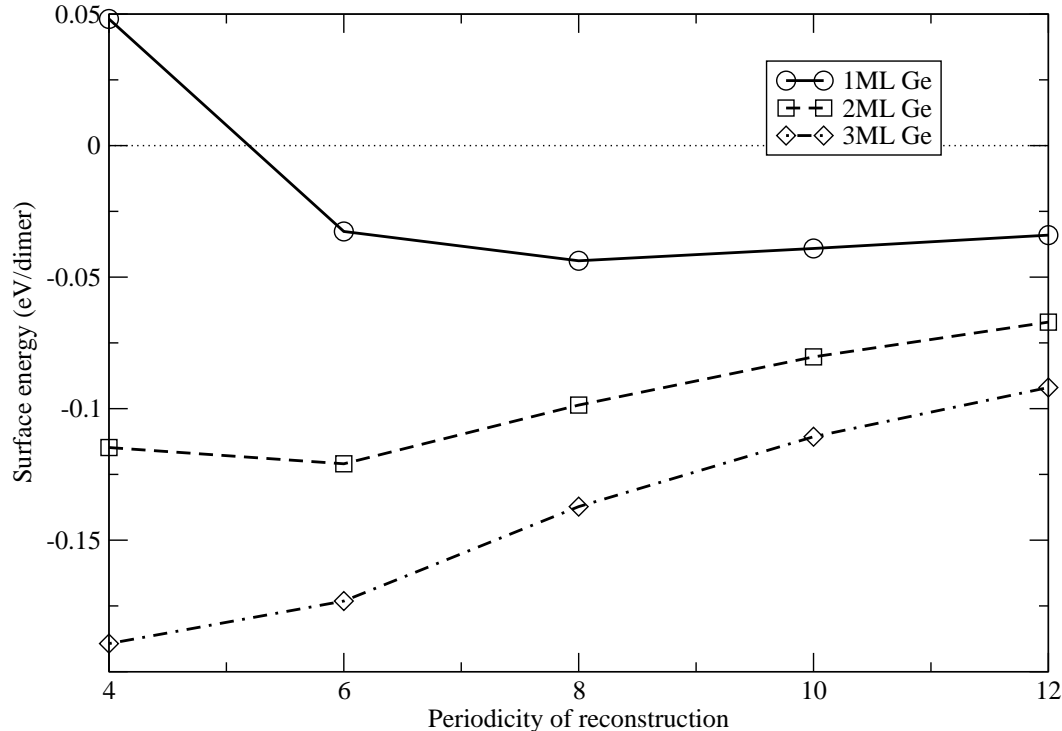


Fig. 3. The surface energy per Ge dimer for the $(2 \times N)$ Ge/Si(001) surface plotted against N for 1, 2 and 3ML coverages.

configuration and a perfect trench.

We assume that only the top layer of Ge is defective, and use the optimal value of N for each system as calculated in section 3.1. We have performed kinking calculations on unit cells with two, four and six dimer rows, in order to find the interaction between adjacent kinks (i.e. in the two dimer row cell, the kinks will be as close as possible, while in the six dimer row cell, they will be separated by three dimer rows each). This effect has been found to be small.

The trench kinking energy of different depths of Ge coverage (1, 2 and 3ML) is shown in table 2. To give an idea of how likely kinks of different depths are, we have also calculated the distribution of the trench kink depths at 600°C, assuming that these are distributed in thermal equilibrium. We have take the probability of a given kink depth, l , at any site to be given by a Boltzmann factor, $P_l \propto e^{E_l/k_B T}$, and have normalised the distribution to obtain a proportion of depths:

$$\sum_l e^{E_l/k_B T} = 1. \quad (2)$$

We can see that at all coverages, a straight trench (kink depth of zero) is most energetically favorable, becoming more so as the depth of Ge (and hence

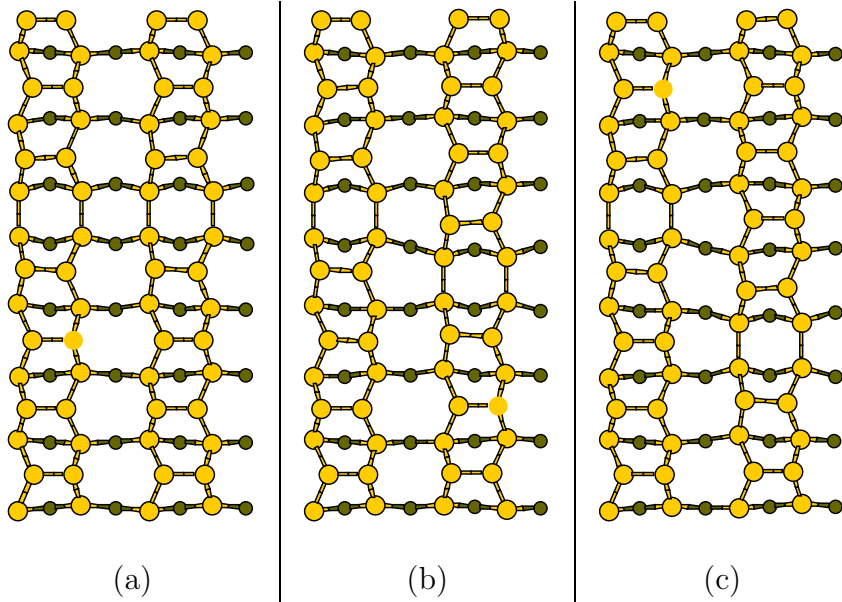


Fig. 4. Kinking in missing dimer trenches for two monolayers of Ge on Si(001). Ge is shown as light circles, Si as dark circles. (a) A missing dimer trench with no kink. (b) A kink of depth one in a missing dimer trench (in the right-hand dimer row, the missing dimer is displaced vertically by one dimer). (c) A kink of depth two in a missing dimer trench (the missing dimer is displaced vertically by two dimers)

strain) increases. For a depth of 1ML of Ge, 45% of trench sites will kink, leading to the highly disordered appearance seen in STM. As the coverage increases, the probability of kinking decreases, so that at 3ML only about 6% of trench sites will kink by 2, and 72% of kink sites will remain straight. It is interesting to note that at all coverages the energy *difference* from a kink depth of 1 to 2 is larger than from a kink depth of 0 to 1, suggesting that there is a strong strain along the trench. Looking at Fig. 4, we can see this strain in the third layer silicon atoms (shown as dark circles) which are significantly more twisted in (c) than in (a). This is orthogonal to the strain that we have seen previously which was *along* the dimer row. These results emphasise the important role that strain plays in the morphologies of the $(2 \times N)$ reconstructed surface in the process of growing Ge/Si(001).

3.3 The $(M \times N)$ reconstruction

Having considered the $(2 \times N)$ reconstruction for multiple layers of Ge, we now move on to the two-dimensional $(M \times N)$ reconstruction (or the “patch” reconstruction), for 2 and 3 ML coverage of Ge, illustrated in Fig. 1 for 2 ML of Ge. For the case of 2 ML of Ge, we fixed N at 8 (from our previous calculation for a single monolayer) and changed the value M to find the most energetically favorable. We used the method described in Sec. 2.2 to calculate $\zeta(M)$ for the $(8 \times M)$ reconstruction, with $E_{\text{pstrip}}(\theta) = -10.03$ eV. These

Table 2

Trench kinking energy of $(2 \times N)$ reconstructed Si(100) with 1, 2 and 3 Ge ML coverage, and kink distribution of kink depth. The temperature considered here is 600°C.

kink depth	θ_{Ge} (ML)	Kink energy(eV)	Population
0	1	0.000	0.554
1	1	0.036	0.348
2	1	0.132	0.098
0	2	0.000	0.645
1	2	0.069	0.258
2	2	0.142	0.097
0	3	0.000	0.717
1	3	0.089	0.219
2	3	0.182	0.064

Table 3

$\zeta(M)$ for the $(M \times N)$ reconstruction at 2 and 3ML of Ge coverage (for a definition of $\zeta(M)$, see Sec. 2.2). The value of N was fixed at 8 (2ML) and 6 (3ML) in accordance with results for the $(2 \times N)$ reconstruction in Sec. 3.1.

	θ_{Ge} (ML)	4	6	8	10
$\zeta(M)$	2	-0.199	-0.262	-0.202	-0.178
$\zeta(M)$	3	-0.275	-0.271	-0.216	-0.175

results are presented in table 3. We can see that the optimal M is 6, that is, of $(8 \times M)$ reconstructions, the (8×6) is most energetically favorable and most stable structure. When modelling the 3 Ge ML coverage case, we used a periodicity of 6 for N (again, considering our earlier results for the $(2 \times N)$ surface with 2 Ge ML) and $E_{pstrip}(\theta) = -10.02$ eV. As shown also in table 3, we found that the optimal M for $(6 \times M)$ reconstruction is between 4 and 6. From these results we can see that the $(M \times N)$ reconstruction is still an effective strain relief mechanism, and that for three layers of Ge more relief is obtained (since the value of $\zeta(M)$ is more negative).

3.4 Comparing the $(2 \times N)$ and $(M \times N)$ reconstructions

We have discussed in Sec. 2.2 how we will compare the stabilities of the $(2 \times N)$ and $(M \times N)$ reconstructions relative to the perfect surface, and these results are given in table 4. We used values of $E_p(\theta)$ and $E_{pstrip}(\theta)$ given above in Sections 3.1 and 3.3 to calculate these energies.

Table 4

Energy per dimer per dimer row relative to perfect layers for $(2 \times N)$ and $(M \times N)$ reconstructions for 2 and 3 layers of Ge on Si(001), given in eV/dimer/dimer row. The final three columns represent the value of N for the $(2 \times N)$ reconstruction and M for the $(M \times N)$ reconstruction. For the $(M \times N)$ reconstruction, the value of N is given in the first column.

Reconstruction	θ_{Ge} (ML)	4	6	8
$(2 \times N)$	2	-0.0862	-0.1008	-0.0862
$(M \times N)(N = 8)$	2	-0.0048	-0.0233	-0.0135
$(2 \times N)$	3	-0.1420	-0.1444	-0.1201
$(M \times N)(N = 6)$	3	-0.0970	-0.1062	-0.0952
$(M \times N)(N = 8)$	3	-0.1220	-0.1284	-0.1134

We see that the $(2 \times N)$ reconstruction is more stable than the $(M \times N)$ for a 2ML coverage of Ge, and also for 3ML though by a much smaller margin. It is interesting that the stability of the $(M \times N)$ reconstructions for 3ML is increased when the second layer has a periodicity of $N = 8$ (though the most stable periodicity for the $(2 \times N)$ reconstruction with two layers of Ge is $N = 6$). Nevertheless, these reconstructions are all stable relative to a perfect surface, and their formation under different growth conditions will depend on a subtle interplay of factors, such as: deposition rate; substrate temperature; and growth source.

4 Conclusions

Various important results can be drawn from our modelling of several layers of Ge on Si(001). First, we have shown that tight binding, and in particular $\mathcal{O}(N)$ tight binding, is sufficiently accurate to be used for modelling complex, strain-driven reconstructions such as those found in this system. Second, we have identified the trends behind the $(2 \times N)$ reconstruction with increasing Ge depth, and shown that the trenches of missing dimers will tend to line up and straighten as the depth of Ge deposited increases. Third, we have explored the $(M \times N)$ “patch” reconstruction for different Ge coverages, contrasting it with the $(2 \times N)$ reconstruction, and shown that, while it is less stable than the $(2 \times N)$ reconstruction for all coverages of Ge considered, it becomes less unstable as the depth of Ge deposited increases.

Our results are based on two fundamental assumptions: full thermal equilibrium; and a lack of intermixing. We have already seen one area where our results appear not to be in exact agreement with experiment (in the value of N for the $(2 \times N)$ reconstruction), and it is quite possible that these assumptions

may be partly responsible for this discrepancy. The experimental observations generally take place on substrates which roughen as growth proceeds, leading to finite domains, which will have a considerable effect on the values of N observed. The values of M found for the $(M \times N)$ reconstruction show a similar trend towards values of $M = 4$, though not as sharply (the value of $M = 6$ for three layers of Ge is essentially degenerate with the value of $M = 4$). At this size of reconstruction, some of the forces governing stability are due to the elastic constants of the system, which tight binding may not reproduce exactly. Nevertheless, our results reproduce and explain observed trends rather well, and may be considered as a limiting case, where the simplest assumptions apply: thermal equilibrium and complete Ge/Si segregation.

Acknowledgements

We thank the UK Engineering and Physical Sciences Research Council and the Royal Society (DRB) and the Chinese Government (KHL) for funding. We gratefully acknowledge useful conversations with Jaime Oviedo, Ilan Goldfarb and James Owen.

References

- [1] Y.-W.Mo, M.G.Lagally, *J. Crystal Growth* 111 (1991) 876.
- [2] J.Oviedo, D.R.Bowler, M.J.Gillan, *Surf. Sci.* 515 (2002) 483.
- [3] I.Goldfarb, J.H.G.Owen, P.T.Hayden, D.R.Bowler, K.Miki, G.A.D.Briggs, *Surf. Sci.* 394 (1997) 105.
- [4] B.Voigtländer, M.Kästner, *Phys. Rev. B* 60 (1999) R5121.
- [5] F.Wu, X.Chen, Z.Zhang, M.G.Lagally, *Phys. Rev. Lett.* 74 (1995) 574.
- [6] K.-H.Huang, T.-S.Ku, D.-S.Lin, *Phys. Rev. B* 56 (1997) 4878.
- [7] U.Köhler, O.Jusko, B.Müller, M. von Hoegen, M.Pook, *Ultramicroscopy* 42-44 (1992) 832.
- [8] M.Tomitori, K.Watanabe, M.Kobayashi, O.Nishikawa, *Appl. Surf. Sci.* 76-77 (1994) 322.
- [9] I.Goldfarb, P.T.Hayden, J.H.G.Owen, G.A.D.Briggs, *Phys. Rev. Lett.* 78 (1997) 3959.
- [10] S.Goedecker, *Rev. Mod. Phys.* 71 (1999) 1085.
- [11] J.Tersoff, *Phys. Rev. B* 43 (1991) 9377.

- [12] J.Tersoff, Phys. Rev. B 45 (1992) 8833.
- [13] F.Liu, M.G.Lagally, Phys. Rev. Lett. 76 (1996) 3156.
- [14] B.P.Uberuaga, M.Leskovar, A.P.Smith, H.Jónsson, M.Olmstead, Phys. Rev. Lett. 84 (2000) 2441.
- [15] C.M.Goringe, D.R.Bowler, E.H.Hernández, Rep. Prog. Phys. 60 (1997) 1447.
- [16] D.R.Bowler, M.Fearn, C.M.Goringe, A.P.Horsfield, D.G.Pettifor, J. Phys.: Condens. Matter 10 (1998) 3719.
- [17] D.R.Bowler, J. Phys.:Condens. Matt. 14 (2002) 4527.
- [18] C.M.Goringe, Computational modelling of semiconductor surfaces, Ph.D. thesis, Oxford University (1995).
URL <http://www.cmp.ucl.ac.uk/~drb/DensEl.html>
- [19] X.-P.Li, R.W.Nunes, D.Vanderbilt, Phys. Rev. B 47 (1993) 10891.
- [20] H.J.Monkhorst, J.D.Pack, Phys. Rev. B 13 (1976) 5188.
- [21] D.R.Bowler, M.Aoki, C.M.Goringe, A.P.Horsfield, D.G.Pettifor, Modell. Simul. Mat. Sci. Eng. 5 (1997) 199.